International Journal of Pharmaceutics: X 2 (2020) 100051

Contents lists available at ScienceDirect

International Journal of Pharmaceutics: X

journal homepage: www.journals.elsevier.com/international-journal-of-pharmaceutics-x

Specific protein-protein interactions limit the cutaneous iontophoretic transport of interferon beta-1B and a poly-ARG interferon beta-1B analogue

S. Dubey[a,b,c], R. Perozzo[a,b], L. Scapozza[a,b], Y.N. Kalia[a,b,*]

[a] School of Pharmaceutical Sciences, University of Geneva, CMU – 1 rue Michel Servet, 1211 Geneva, Switzerland
[b] Institute of Pharmaceutical Sciences of Western Switzerland, University of Geneva, CMU - 1 Rue Michel Servet, 1211 Geneva, Switzerland
[c] Ichnos Sciences S.A., Chemin de la Combeta 5, 2300 La Chaux-de-Fonds, Switzerland

ARTICLE INFO

Keywords:
Transdermal iontophoresis
Interferon (IFN)
Protein delivery
Protein interaction
Electromigration
Electroosmosis
Albumin

ABSTRACT

The first objective was to investigate the transdermal iontophoresis of interferon beta 1b (IFN); the second was to determine whether the addition of 10 Arg residues at the N-terminus, creating a highly charged poly-Arg analogue (Arg_{10}-IFN), increased delivery. Cumulative permeation of IFN and Arg_{10}-IFN after iontophoresis at 0.5 mA/cm^2 for 8 h was 6.97 ± 4.82 and 9.55 ± 1.63 ng/cm^2, respectively – i.e. > 1000-fold less than that of ribonuclease A, cytochrome *c* and human basic fibroblast growth factor. Co-iontophoresis of acetaminophen showed that, in contrast to lysozyme, neither IFN nor Arg_{10}-IFN interacted with skin to decrease convective solvent flow. Furthermore, there was no statistically significant difference between (i) iontophoretic delivery of IFN across intact or laser porated skin and (ii) passive or iontophoretic delivery of IFN across laser porated skin. Chromatographic characterisation supported the hypothesis that IFN was bound strongly to albumin. The formation of a ~ 86 kDa complex with albumin was probably responsible for the poor cutaneous delivery of IFN/Arg_{10}-IFN despite the use of iontophoresis and/or laser microporation. Biopharmaceuticals might interact with specific proteins during iontophoretic transport and so decrease their (per)cutaneous delivery without affecting electroosmotic solvent flow, which is usually considered as a reliable marker to report on permeant binding during electrotransport across the skin.

1. Introduction

Biopharmaceuticals have gained importance over the last two decades with approximately a quarter of all new molecules approved by the US FDA being of biological origin (Mullard, 2020). Significant progress has been made in the development of new and complex molecular formats; however, their delivery has largely been restricted to intravenous (IV) infusion or subcutaneous (SC) injections (Nongkhlaw et al., 2020). Different delivery options for proteins have been explored including transdermal administration. However, the skin is a very efficient biological and diffusional barrier against external agents (Naik et al., 2000) and it is particularly effective against the transport of large hydrophilic molecules – the rate and extent of their transport by passive diffusion are insufficient for therapeutic applications. Several methods have been evaluated in an effort to improve transdermal delivery of macromolecules (Anselmo et al., 2019) including ablative methods – e.g. laser microporation (Yu et al., 2011; Lapteva et al., 2019; Del Río-Sancho et al., 2020), which has also been used to deliver cells (Yu et al., 2018) – or the use of microneedles (Dharadhar et al., 2019) – and non-invasive techniques such as iontophoresis (Cazares-Delgadillo et al., 2007; Dubey and Kalia, 2010; Dubey and Kalia, 2011; Dubey et al., 2011). In addition to being a non-invasive and active transport process, iontophoresis enables complex input kinetics that mimic endogenous secretion/release profiles, e.g. pulsatile liberation of gonadotropin releasing hormone (GnRH), and thereby offers a potentially more convenient alternative to IV infusion (Kalia et al., 2004). Furthermore, transdermal iontophoresis is also one of the approaches that has resulted in approved therapeutic products (Kalaria et al., 2012).

It has previously been shown that transdermal iontophoresis can be used for the non-invasive delivery across the skin of medium-sized proteins (cytochrome *c* (Cyt c; 12.4 kDa), ribonuclease A (RNase A; 13.7 kDa), ribonuclease T1 (RNase T1; 11.1 kDa) and human basic fibroblast growth factor (hbFGF; 17.4 kDa) across intact skin (Cazares-Delgadillo et al., 2007; Dubey and Kalia, 2010; Dubey and Kalia, 2011; Dubey et al., 2011). Indeed, it was also recently demonstrated that iontophoresis was able to deliver an intact antibody, cetuximab, into the skin (Lapteva et al., 2020). Moreover, it was also demonstrated that biological activity of proteins was retained post-delivery since

* Corresponding author at:School of Pharmaceutical Sciences, University of Geneva, CMU – 1 rue Michel Servet, 1211 Geneva, Switzerland.
E-mail address: yogi.kalia@unige.ch (Y.N. Kalia).

https://doi.org/10.1016/j.ijpx.2020.100051
Received 10 June 2020; Received in revised form 2 July 2020; Accepted 4 July 2020
Available online 08 July 2020

quantification of the amounts delivered could be performed using activity-based assays (Dubey and Kalia, 2010; Dubey and Kalia, 2011; Dubey et al., 2011).

However, proteins with superficially similar physicochemical properties (i.e. molecular weight, pI, electric mobility) can have very different electrotransport behaviour. This was demonstrated by a study into the iontophoresis of lysozyme, which has a higher electric mobility than cytochrome *c* but whose delivery is almost 200-fold lower (Dubey and Kalia, 2014). In that case, it appeared that lysozyme interacted strongly with fixed negative charged sites in the skin causing a significant reduction in the electroosmotic solvent flow. This behaviour had been observed previously for small molecules (Hirvonen et al., 1996), peptides (Delgado-Charro and Guy, 1994; Schuetz et al., 2005) and long-chain polylysines (Hirvonen and Guy, 1998). In addition, the results suggested that the surface hydrophobicity of lysozyme might also have facilitated other protein-skin interactions.

The first objective of the present study was to investigate the iontophoretic delivery of a biopharmaceutical, interferon beta-1b (IFN; 166 amino acids, 20.0 kDa), a medium-sized protein that is used in the treatment of multiple sclerosis. It has a predominantly helical structure and a pI of 8.78 (PDB: 1AU1) (Karpusas et al., 1997) and a net positive charge of +5 at neutral pH (http://protcalc.sourceforge.net/). The second aim was to determine whether modification of the amino acid sequence through the addition of 10 Arg residues at the N-terminus – creating a highly positively charged poly-Arg analogue (Arg_{10}-IFN) – was able to enhance transdermal electrotransport. Given the results of the lysozyme study and the earlier studies investigating the iontophoretic transport of high molecular weight polylysines across hairless mouse skin (Hirvonen and Guy, 1998), the potential of IFN and Arg_{10}-IFN to bind to skin and so neutralise the skin's net negative charge and decrease convective solvent flow was reported on by co-iontophoresis of acetaminophen (Padula et al., 2005; Schuetz et al., 2005). The iontophoretic transport of IFN was also compared across intact and laser porated skin to see whether the creation of micropores was able to facilitate electrically-assisted delivery (Badkar et al., 2007).

2. Materials and methods

2.1. Chemicals and reagents

Interferon beta-1b (IFN, Betaseron®; Bayer) was purchased from the hospital pharmacy in Geneva University Hospital (HUG; Geneva, Switzerland). Arg_{10}-IFN (interferon beta-1b with 10 Arg residues inserted at the N-terminus) was cloned, expressed and purified in-house (see below). The *ifn* gene (Ultimate ORF Clone; Ref No. IOH35219), pET100/D-TOPO® cloning kit, dNTP mix, and chemo-competent BL21(DE3)-Star cells were obtained from Invitrogen (Carlsbad, CA). Rosetta™ (DE3) cells were obtained from Novagen (Darmstadt, Germany). Primers were synthesised by Microsynth (Balgach, Switzerland). Isopropyl β-D-1-thiogalactopyranoside (IPTG) and imidazole were purchased from Applichem (Darmstadt, Germany). Yeast extract and tryptone were purchased from Becton Dickinson and Company (Le Pont de Claix, France). The ELISA kit (product number 41415–1) used for the quantification of IFN and Arg_{10}-IFN was purchased from PBL Interferon Source (Piscataway, NJ). Acetaminophen (ACM), Tris®, silver wire and silver chloride were purchased from Sigma-Aldrich (Buchs, Switzerland). 4-(2-hydroxyethyl)-1-piperazineethanesulfonic acid) (HEPES) was purchased from Acros Organics (Chemie Brunschwig; Basel, Switzerland). PVC tubing (3 mm ID, 5 mm OD, 1 mm wall thickness) used to prepare salt bridge assemblies was obtained from Fisher Bioblock Scientific S.A. (Illkirch, France). All solutions were prepared using deionised reverse osmosis filtered water (resistivity ≥18 MΩ.cm). All other chemicals were at least of analytical grade.

2.2. Cloning, expression and purification of Arg_{10}-IFN

The IFN was amplified from a commercially purchased gene (Ultimate ORF Clone; Ref No. IOH35219; Invitrogen) by PCR (Sambrook et al., 1989). The forward and reverse primers were CACC *CTGGTGCCGCGCGGCAGC***CGCCGTCGCCGTCGCCGTCGCCGTCGCCG** TATGAGCTACAACTTGCTT and AAGAATTCTCAGTTTCGGAGGTAACC TGTAAGTC, respectively. A thrombin cleavage site (sequence in italics) and 10 Arg residues (sequence in bold) were introduced upstream of the *ifn* gene. PCR amplified product (~500 bp) was introduced into the pET100/D-TOPO expression vector following the protocol provided by the supplier. The plasmid was transformed into competent BL21(DE3)-Star cells. The plasmid was re-isolated for sequence verification and the sequence verified clone was used for site directed mutagenesis (SDM), which was carried out to replace the Cys at position 17 by a Ser as in Interferon beta 1b (IFN). Forward and reverse primers used for SDM were CTACAAAGAAGCAGCAATTTTCAGTCTCAGAAGCTCCTGTGGCA ATTG and CAATTGCCACAGGAGCTTCTGAGACTGAAAATTGCTGCTTC TTTGTAG, respectively. This plasmid was transformed into competent Rosetta™ (DE3) cells.

Expression of Arg_{10}-IFN was carried out in 1 l LB medium (0.5% yeast extract, 1% tryptone and 1% NaCl) containing 100 μg/ml ampicillin and 170 μg/ml chloramphenicol. IPTG (1 mM) was added to the *E. coli* (grown overnight at 37 °C) culture after cooling the culture broth to 12 °C. Expression was continued for 3 days, before harvesting the cells. The protein was purified in three steps; the first involved Ni-affinity chromatography (HiTrap™ 5 ml column) using 20 mM Tris buffer pH 8 and elution was achieved using a 500 mM imidazole gradient. This was followed by thrombin digestion overnight at 16 °C. Cation exchange chromatography (HiTrap™ (IEX) SP HP (5 ml)) at pH 7.8 (100 mM phosphate buffer; gradient of 1 M NaCl) was used to purify the protein further and to remove thrombin. Finally, the protein was eluted through a size exclusion column (Superdex-75 10/300 GL) (using 0.54% NaCl solution and 15 mg/ml mannitol). After elution, BSA (15 mg/ml; instead of HSA as in Betaseron®) was added to the Arg_{10}-IFN to provide stability.

2.3. Skin source

Porcine ears were obtained from a local abattoir (CARRE; Rolle, Switzerland), the skin was excised (thickness 250 μm) with an air dermatome (Zimmer; Etupes, France), wrapped in Parafilm™ and stored at −20 °C for a maximum period of 2 months.

2.4. Stability studies

Protein stability in the presence of epidermis, dermis and current was performed as described previously (Cazares-Delgadillo et al., 2007; Dubey and Kalia, 2010). The concentration of IFN was kept at 250 μg/ml and a sample was taken after incubation for 8 h.

2.5. Transport studies

Permeation experiments were performed using two-compartment vertical diffusion cells (area ~ 2.0 cm^2) equipped with an additional sampling arm in the receptor compartment; dermatomed skin was clamped between the donor and receptor compartments. The anode (containing 25 mM HEPES, 133 mM NaCl, pH 7.4) was connected to the formulation via a salt bridge assembly (3% agarose in 0.1 M NaCl) (Cazares-Delgadillo et al., 2007; Dubey et al., 2011). After equilibration for 40 min with 25 mM HEPES, 133 mM NaCl (pH 7.4), the buffer solution in the donor compartment was replaced with 1 ml of protein solution (250 μg/ml of either IFN – using the Betaseron® formulation as supplied – or Arg_{10}-IFN with 15 mM acetaminophen). The receptor compartment was filled with 12 ml of 25 mM HEPES, 133 mM NaCl, pH 7.4 solution. Constant current (0.5 mA/cm^2) was applied using Ag/

AgCl electrodes connected to a power supply (Kepco® APH 1000 M, Flushing, NY).

Laser poration was performed using the P.L.E.A.S.E.® system (Precise Laser Epidermal System; Pantec Biosolutions AG; Ruggell, Liechtenstein); the pore density was 300 pores per cm^2 and the fluence was 18.7 J/cm^2 (Bachhav et al., 2010; Bachhav et al., 2013). Samples were taken from the receiver compartment after completion of the permeation experiment (8 h). The amount of protein deposited in the skin during current application was determined by first cutting the skin samples into small pieces and then stirring them in 10 ml of an extraction medium (25 mM HEPES, 133 mM NaCl, pH 7.4 buffer) for 18 h. The resulting extract was filtered through 0.45 μm membrane filters and the filtrate was used for quantification. All samples were analysed by using a commercial ELISA kit (details below).

2.6. Quantification of IFN and Arg_{10}-IFN

IFN and Arg_{10}-IFN were quantified using a commercial ELISA kit (*VeriKine*-HS™ Human IFN-β Serum ELISA kit (# 41415–1), PBL Interferon Source; Piscataway, NJ) following the protocol provided by the supplier. Briefly, 50 μl of sample buffer, appropriately diluted antibody solution and sample (standards and test samples) were pipetted into a 96-well ELISA plate. The plate was sealed and incubated at room temperature for 2 h. The plate was washed and 100 μl of HRP-conjugated secondary antibody was added. After incubation at room temperature for 30 min, the plate was again washed and TMB substrate solution (100 μl) was added. The reaction was stopped after another 30 min by the addition of stop solution (100 μl). The absorbance was read at 450 nm immediately after terminating the reaction. The LOD and LOQ were 17.1 and 51.7 pg/ml, respectively.

2.7. Quantification of acetaminophen

Acetaminophen was analysed using a P680A LPG-4 pump equipped with an ASI-100 autosampler and a UV/Vis detector (UVD 170 U) (Dionex, Voisins LeBretonneux, France) and a Lichrospher® column packed with 5 μm C18 silica reversed-phase particles. The mobile phase comprised 80% citrate buffer (40 mM; pH 3.0) and 20% methanol. The flow rate was 1 ml/min, the column temperature was 30 °C and the injection volume was 25 μl. ACM was detected using its absorbance at 243 nm. The LOD and LOQ were 0.16 and 0.49 μg/ml, respectively.

2.8. Chromatographic characterisation of IFN

IFN was characterised by using a Fast Protein Liquid Chromatography system (AKTA purifier; Amersham). A HiTrap™ (IEX) SP HP (5 ml) column was used for cation exchange chromatography with a flow rate of 4 ml/min and a gradient from 0 to 100% in 20 column volumes. Buffer A comprised 0.1 M phosphate (pH 6.4) while buffer B contained 1 M NaCl in 0.1 M phosphate (pH 6.4). In a second set of experiments, a Superdex 75 10/300 GL column was used for size exclusion chromatography. The flow rate was 0.5 ml/min and the elution buffer was 0.1 M phosphate (pH 7.4).

2.9. Statistical analysis

Data were expressed as mean ± SD. Outliers determined using the *Grubbs* test were discarded. Results were evaluated statistically using analysis of variance (ANOVA) or *Student's t-test*. The level of significance was fixed at $\alpha = 0.05$.

3. Results and discussion

3.1. Production of Arg_{10}-IFN

Positive clones were identified by PCR and restriction digestion. The sequence of the insert was verified by automated sequencing to ensure the correct insertion of the *ifn* gene. After SDM, automated sequencing was again used to confirm the replacement of Cys by Ser at position 17. Soluble protein was purified in three steps; first, Ni-affinity chromatography was used to separate Arg_{10}-IFN from native *E. coli* proteins. Arg_{10}-IFN eluted at ~30% imidazole concentration, fractions were pooled and were incubated with thrombin (10 U enzyme per ml of protein solution) for 16 h at 16 °C to cleave the His_6-tag. The protein was further purified using cation-exchange chromatography at pH 7.8. At this pH, Arg_{10}-IFN, by virtue of its high pI (10.04) was bound to the column whereas thrombin and other fragmented products were not. In the final step, Arg_{10}-IFN was purified on a size exclusion column in order to change the buffer and have a formulation as close as possible to that of Betaseron®. After elution, BSA (15 mg/ml; instead of HSA as in Betaseron®) was added to the Arg_{10}-IFN. MALDI-TOF analysis before thrombin cleavage gave a molecular weight of 26,404 Da (predicted MW: 26308 Da), indicating that intact Arg_{10}-IFN had been expressed (the difference in MW of 96 Da was attributed to TFA). The protein was analysed by Western blot (Burnette, 1981); the two neighbouring bands observed between the 17 and 28 kDa markers represented Arg_{10}-IFN before and after thrombin cleavage.

3.2. Stability studies

The IFN concentration measured in solution after 8 h in the presence of epidermis, dermis and following current application (0.5 mA/cm^2) was 100.13 ± 0.66, 97.89 ± 4.20 and 97.19 ± 5.70%, respectively of the initial value. The corresponding values for Arg_{10}-IFN were 100.04 ± 0.71, 97.31 ± 2.96 and 91.83 ± 7.02% confirming that the analogue had similar stability to IFN.

3.3. Iontophoretic transport studies

Cumulative permeation and skin deposition of IFN after iontophoresis for 8 h at 0.5 mA/cm^2 were 6.97 ± 4.82 and 293.15 ± 3.12 ng/cm^2, respectively (Table 1). These amounts were approximately 1000-fold less than the quantities observed in previous studies with Cyt c, RNase A and hbFGF under similar conditions (Cazares-Delgadillo et al., 2007; Dubey and Kalia, 2010; Dubey et al., 2011) and furthermore, they were also ~10-fold lower than the corresponding values for lysozyme (Dubey and Kalia, 2014). Given the lower net positive charge of IFN (+5) as compared to Cyt c (+7.9), RNase A (+7.2) and hbFGF (+10), it might have been considered that

Table 1
Permeation and skin deposition of IFN and Arg10-IFN.

	Permeation (ng/cm^2)	Deposition (ng/cm^2)	Iontophoretic permeability coefficient[a] (cm/h)
IFN	6.97 ± 4.82	293.16 ± 3.12	3.49×10^{-6}
Arg_{10}-IFN	9.55 ± 1.63	87.85 ± 14.15	4.78×10^{-6}

[a] Iontophoretic permeability coefficient was calculated by dividing cumulative permeated amount by the time of delivery experiment (8 h). Iontophoretic permeability coefficient as calculated from previously reported data for RNase A and hbFGF is 5.55 and 9.30×10^{-3} cm/h, respectively (Dubey and Kalia, 2011; Dubey et al., 2011). Thus, representing an almost 1000-fold difference.

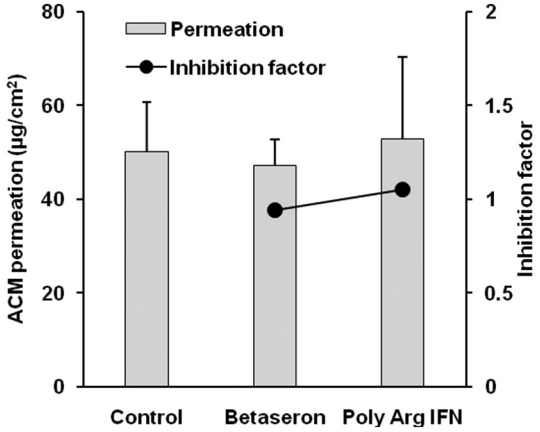

Fig. 1. Cumulative acetaminophen (ACM) permeation across porcine skin after 8 h of iontophoresis at 0.5 mA/cm^2 (control, Betaseron® (IFN) and Poly Arg IFN (Arg_{10}-IFN), filled circles show the inhibition factor; values of ~1 confirm the absence of electroosmosis inhibition. (Mean ± SD; $n \geq 4$).

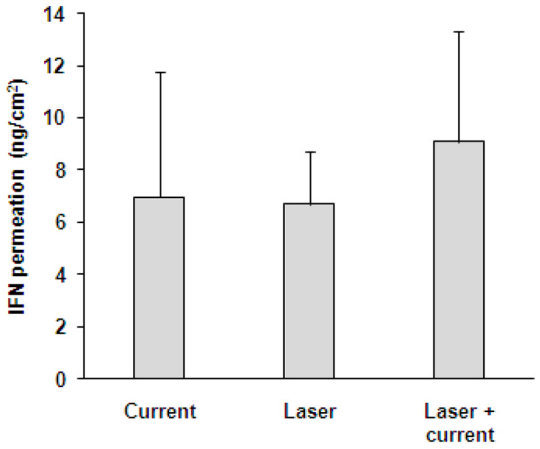

Fig. 2. Comparison of IFN iontophoretic permeation across intact and laser porated porcine skin after 8 h; results of passive IFN permeation across laser porated skin are also shown. (Mean ± SD; n ≥ 4).

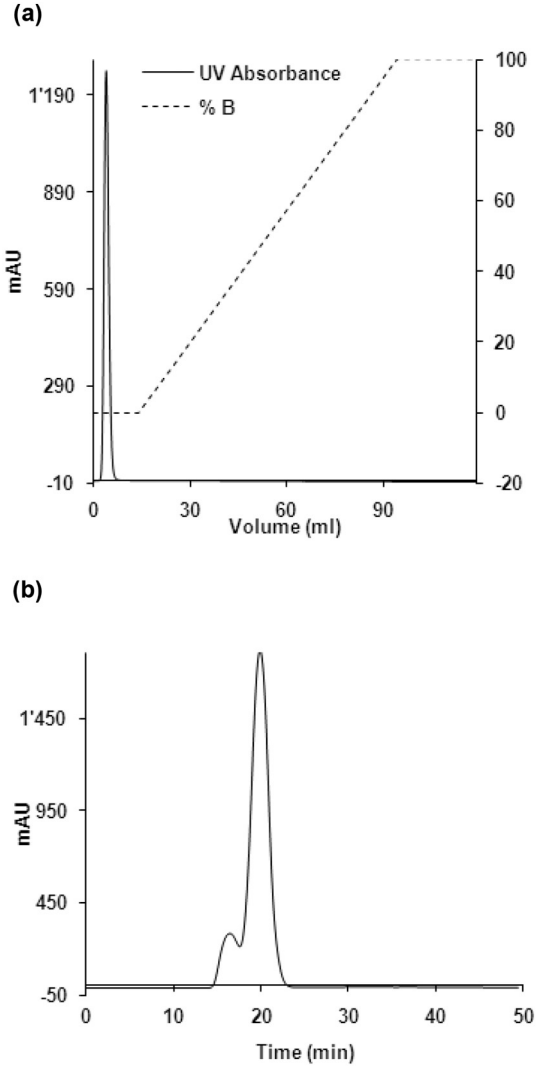

Fig. 3. (a) Cation exchange chromatography of IFN; the presence of a single peak during the flow through and the absence of any peak during gradient application (from 0 to 100%) suggests that there is a strong interaction between HSA and IFN. (b) Size exclusion chromatography; a non-resolvable shoulder peak at 16.5 min might be due to the HSA-IFN complex. The absence of any peak at ~26 min confirms the absence of free IFN in the solution.

this contributed to its poorer delivery. However, the iontophoretic transport of Arg_{10}-IFN with its 10 additional Arg residues and net charge of +15 was no better; cumulative permeation was 9.55 ± 1.63 ng/cm^2 with no statistically significant difference to that of IFN (*Student's t-test;* α = 0.05) and, indeed, skin deposition was lower (87.85 ± 14.14 ng/cm^2) (Table 1).

Thus, it was hypothesised that, given their positive charge, IFN and Arg_{10}-IFN might be binding to fixed negatively charged sites in the skin as seen for other small molecules and peptides (Delgado-Charro and Guy, 1994; Hirvonen et al., 1996; Hirvonen et al., 1998; Schuetz et al., 2005; Dubey and Kalia, 2014). However, co-iontophoresis of ACM revealed that electroosmotic flow was unaffected by the co-iontophoresis of either IFN or Arg_{10}-IFN (ANOVA (α = 0.05); cumulative ACM permeation was 47.23 ± 5.42, 52.74 ± 17.68 and 50.14 ± 10.51 µg/cm^2 in the presence of IFN, Arg_{10}-IFN and in the control (no protein; only acetaminophen), respectively (Fig. 1).

3.4. Effect of laser microporation on passive and iontophoretic delivery of IFN

Despite the fact that neither IFN nor Arg_{10}-IFN appeared to bind to the negatively charged sites in the skin (as evidenced by the lack of effect on ACM transport), it was thought that the proteins might be binding to other sites in the stratum corneum. Therefore, in the next series of experiments, the stratum corneum was subjected to fractional laser ablation using the P.L.E.A.S.E.® Er.YAG device, which had been used in earlier studies to enhance the transport of similarly sized proteins – cytochrome *c* (12.4 kDa), human growth hormone (22 kDa), follicle stimulating hormone (30 kDa) (Bachhav et al., 2013). However, comparison of IFN iontophoretic transport across intact and laser-porated skin samples revealed that cumulative iontophoretic permeation was statistically equivalent (cf. 6.97 ± 4.82 and 9.10 ± 4.19 ng/cm^2, respectively). Furthermore, the combination of iontophoresis and laser poration was not superior to laser poration alone (6.69 ± 2.04 and 9.10 ± 4.19 ng/cm^2, respectively) (Fig. 2) (*Student's t-test;* α = 0.05). Thus, given that (i) IFN / Arg_{10}-IFN electrotransport had no effect on EO flow and (ii) removal of the stratum corneum had no effect on iontophoretic transport of IFN, this suggested that some other type of "interaction" was affecting electrotransport.

3.5. Interaction of IFN with skin proteins

Cation exchange chromatography was performed at pH 6.4 and at this pH IFN is predicted to be positively charged (+6.9; 1AU1; http://

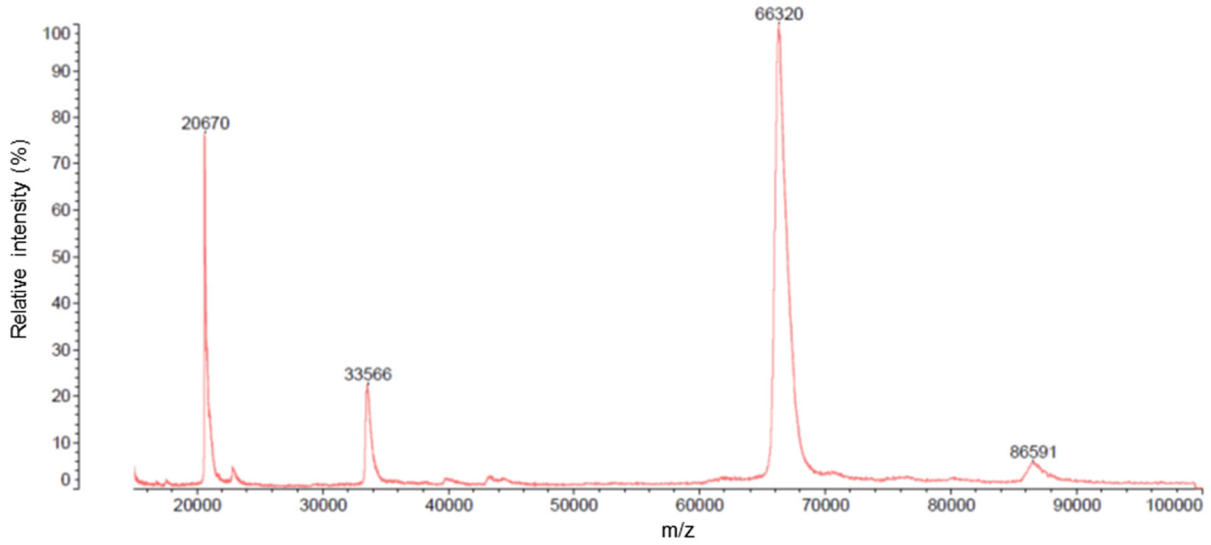

Fig. 4. MALDI-TOF spectra of standard IFN (BetaseronBetaseron® sample) recorded using Axima CFR$^+$ (Shimadzu) in positive mode. Peak of 20,670 Da corresponds to IFN; peak at 66,320 Da corresponds to HSA while peak at 86,591 Da could correspond to IFN-HSA complex.

Table 2
Similarity profile between different proteins; calculated using BlastP ((http://blast.ncbi.nlm.nih.gov/Blast.cgi?PAGE=Proteins) Altschul et al., 1997)). HSA: human serum albumin; PSA: porcine serum albumin; RSA: rat serum albumin; IFN β 1b: Interferon beta 1b and IFN α 2b: Interferon alpha 2b.

	Identity (%)	Similarity (%)	Query coverage (%)	E value
HSA: PSA	76	87	99	0.0
HSA: RSA	74	88	99	0.0
PSA: RSA	73	86	100	0.0
IFN β 1B: IFN α 2B	38	58	81	4E-26

protcalc.sourceforge.net/) (Karpusas et al., 1997). It was noted that the formulation also contained human serum albumin (HSA); at pH 6.4, this is negatively charged (−5.4; 1AO6; http://protcalc.sourceforge.net/) (Sugio et al., 1999). Thus, it was expected that HSA would be seen in the flow through, i.e., in the loading and column washing period before the start of the gradient, while IFN would bind to the column and elute with the gradient. Surprisingly, the only peak observed was during the flow through (Fig. 3a); this indicated that either IFN was bound to the column so strongly that it did not elute even with 1 M NaCl or that it was bound to HSA. It has been shown previously that different IFN variants can bind to albumin (Huang et al., 1974; Braude and Clercq, 1979). Size exclusion chromatography was performed to test this hypothesis. Under the conditions used, IFN was estimated to elute at ~26 min (cf., myoglobin, a similar sized standard (~17 kDa) eluted at ~26 min (chromatogram not shown)). Fig. 3b shows two non-separated peaks at ~16.5 and ~ 20 min (and the absence of any peak at ~26 min); SDS-PAGE analysis (data not shown) of these two peaks revealed that the second peak corresponded to HSA while the first peak consisted of bands corresponding to IFN and HSA. This was confirmed by MALDI-TOF analysis of the Betaseron® formulation (Fig. 4) where an additional peak at 86591 Da was seen, which might correspond to the HSA-IFN interaction product. Thus, it seems clear that there is an interaction between HSA with IFN; given that HSA has high homology with porcine albumin (Table 2) ((http://blast.ncbi.nlm.nih.gov/Blast.cgi?PAGE=Proteins) Altschul et al., 1997), it is likely that the strong interaction with albumin either in the formulation or present in porcine skin might account for the poor delivery of IFN and Arg_{10}-IFN (Fisher, 1964; Fleischmajer and Krol, 1966; Worm et al., 1981). A previous report into the effect of thermal ablation (using the PassPort ™ system developed by Altea Therapeutics) on the transdermal delivery of interferon alpha-2b in hairless rats showed that although iontophoresis produced a ~ 2-fold increase in delivery after 6 h (397 ± 62 and 722 ± 169 ng, respectively), the amounts were significantly below therapeutic levels (Badkar et al., 2007). Those findings may also be explained by the results of the present study since given the homology (Table 2), interferon alpha-2b delivery might also have been hindered by interactions with rat albumin present in the skin (Radhakrishnan et al., 1996).

4. Conclusions

This study provides further evidence that high charge is not an adequate predictor of the feasibility of iontophoretic protein delivery – the highly positively-charged IFN analogue, Arg_{10}-IFN, did not show superior transport to IFN. It also demonstrates that proteins can interact with the skin without impacting electroosmotic solvent flow. Hence, there is no change in the transport of neutral marker molecules, such as acetaminophen and inhibition factors remain close to unity despite the presence of extremely strong interactions that effectively shut down electrotransport. In depth studies using quantitative thermometric analysis and computational tools will help to understand the nature and strength of the interaction between IFN / Arg_{10}-IFN and albumin which may be useful for future formulation development for this and other protein candidates for transdermal delivery.

Author contributions

Y.K.; R.P.; L.S. - Conceptualization; S.D.; R.P. - Formal analysis; Y.K. - Funding acquisition; S.D.; R.P. - Investigation; S.D.; R.P. - Methodology; Y.K. - Project administration; Y.K.; L.S. - Resources; Y.K. - Supervision; S.D.; R.P. - Writing - original draft; All co-authors- Writing - review & editing

Declaration of Competing Interest

The authors declare that they have no known competing financial interests or personal relationships that could have appeared to influence the work reported in this paper.

Acknowledgements

We would like to thank the University of Geneva for a teaching assistantship for SD and we acknowledge Nathalie Oudry and Prof. Gérard Hopfgartner, of the High Resolution Mass Spectrometry Platform, (Faculty of Science, University of Geneva), for the MALDI-TOF analysis. This paper is dedicated to our coauthor and friend, Dr. Remo Perozzo.

References

Altschul, S.F., Madden, T.L., Schaffer, A.A., Zhang, J., Zhang, Z., Miller, W., Lipman, D.J., 1997. Gapped BLAST and PSI-BLAST: a new generation of protein database search programs. Nucleic Acids Res. 25, 3389–3402.

Anselmo, A.C., Gokarn, Y., Mitragotri, S., 2019. Non-invasive delivery strategies for biologics. Nat. Rev. Drug Discov. 18, 19–40.

Bachhav, Y.G., Summer, S., Heinrich, A., Bragagna, T., Bohler, C., Kalia, Y.N., 2010. Effect of controlled laser microporation on drug transport kinetics into and across the skin. J. Control. Release 146, 31–36.

Bachhav, Y.G., Heinrich, A., Kalia, Y.N., 2013. Controlled intra- and transdermal protein delivery using a minimally invasive Erbium: YAG fractional laser ablation technology. Eur. J. Pharm. Biopharm. 84, 355–364.

Badkar, A.V., Smith, A.M., Eppstein, J.A., Banga, A.K., 2007. Transdermal delivery of interferon alpha-2B using microporation and iontophoresis in hairless rats. Pharm. Res. 24, 1389–1395.

Braude, I.A., Clercq, E.D., 1979. Purification of mouse interferon by sequential chromatography. J. Chromatogr. 172, 207–219.

Burnette, W.N., 1981. "Western blotting": electrophoretic transfer of proteins from sodium dodecyl sulfate–polyacrylamide gels to unmodified nitrocellulose and radiographic detection with antibody and radioiodinated protein A. Anal. Biochem. 112, 195–203.

Cazares-Delgadillo, J., Naik, A., Ganem-Rondero, A., Quintanar-Guerrero, D., Kalia, Y.N., 2007. Transdermal delivery of cytochrome C – a 12.4 kDa protein – across intact skin by constant–current iontophoresis. Pharm. Res. 24, 1360–1368.

Del Río-Sancho, S., Lapteva, M., Sonaje, K., Böhler, C., Ling, V., Boehncke, W.-H., Kalia, Y.N., 2020. Targeted cutaneous delivery of etanercept using Er:YAG fractional laser ablation. Int. J. Pharm. 580, 119234.

Delgado-Charro, M.B., Guy, R.H., 1994. Characterization of convective solvent flow during iontophoresis. Pharm. Res. 11, 929–935.

Dharadhar, S., Majumdar, A., Dhoble, S., Patravale, V., 2019. Microneedles for transdermal drug delivery: a systematic review. Drug Dev. Ind. Pharm. 45, 188–201.

Dubey, S., Kalia, Y.N., 2010. Non-invasive iontophoretic delivery of enzymatically active ribonuclease A (13.6 kDa) across intact porcine and human skins. J. Control. Release 145, 203–209.

Dubey, S., Kalia, Y.N., 2011. Electrically-assisted delivery of an anionic protein across intact skin: iontophoresis of biologically active Ribonuclease T1. J. Control. Release 152, 356–362.

Dubey, S., Kalia, Y.N., 2014. Understanding the poor iontophoretic transport of lysozyme across the skin: when high charge and high electrophoretic mobility are not enough. J. Control. Release 183, 35–42.

Dubey, S., Perozzo, R., L. Scapozza, L., Kalia, Y.N., 2011 Non-invasive electrically-assisted transdermal delivery of human basic fibroblast growth factor. Mol. Pharm. 8, 1322–1331.

Fisher, J.P., 1964. Soluble substances of human stratum corneum. J. Invest. Dermatol. 44, 43–50.

Fleischmajer, R., Krol, S., 1966. Non-collagenous proteins of human dermis. J. Invest. Dermatol. 28, 359–363.

Hirvonen, J., Guy, R.H., 1998. Transdermal iontophoresis: modulation of electroosmosis by polypeptides. J. Control. Release 50, 283–289.

Hirvonen, J., Kalia, Y.N., Guy, R.H., 1996. Transdermal delivery of peptides by Iontophoresis. Nat. Biotechnol. 14, 1710–1713.

Huang, J.W., Davey, M.W., Hejna, C.J., Muenchhausen, W.N., Sulkowski, E., Carter, W.A., 1974. Selective binding of human interferon to albumin immobilized on agarose. J. Biol. Chem. 249, 4665–4667.

Kalaria, D.R., Dubey, S., Kalia, Y.N., 2012. Clinical applications of transdermal iontophoresis. In: Watkinson, A.C., Benson, H.A. (Eds.), Topical and Transdermal Drug Delivery and Development. John Wiley & Sons Inc, New Jersey, pp. 67–83.

Kalia, Y.N., Naik, A., Garrison, J., Guy, R.H., 2004. Iontophoretic drug delivery. Adv. Drug Deliv. Rev. 56, 619–658.

Karpusas, M., Nolte, M., Benton, C.B., Meier, W., Lipscomb, W.N., Goelz, S., 1997. The crystal structure of human interferon beta at 2.2-A resolution. Proc. Natl. Acad. Sci. U. S. A. 94, 11813–11818.

Lapteva, M., Del Rio-Sancho, S., Wu, E., Carbonell, W.S., Bohler, C., Kalia, Y.N., 2019. Fractional laser ablation for the targeted cutaneous delivery of an anti-CD29 monoclonal antibody - OS2966. Sci. Rep. 9, 1030.

Lapteva, M., Sallam, M.A., Goyon, A., Guillarme, D., Veuthey, J.L., Kalia, Y.N., 2020. Non-invasive targeted iontophoretic delivery of cetuximab to skin. Expert Opin. Drug Deliv. 17, 589–602.

Mullard, A., 2020. 2019 FDA drug approvals. Nat. Rev. Drug Discov. 19, 79–84.

Naik, A., Kalia, Y.N., Guy, R.H., 2000. Transdermal drug delivery: overcoming the skin's barrier function. Pharm. Technolo. Today 3, 318–326.

Nongkhlaw, R., Patra, P., Chavrasiya, A., Jayabalan, N., Dubey, S., 2020. Biologics: delivery options and formulation strategies. In: Shegokar, R. (Ed.), Drug Delivery Aspects. Elsevier, pp. 115–155.

Padula, C., Sartori, F., Marra, F., Santi, P., 2005. The influence of iontophoresis on acyclovir transport and accumulation in rabbit ear skin. Pharm. Res. 22, 1519–1524.

Radhakrishnan, R., Walter, L.J., Hruza, A., Reichert, P., Trotta, P.P., Nagabhushan, T.L., Walter, M.R., 1996. Zinc mediated dimer of human interferon-alpha 2b revealed by X-ray crystallography. Structure. 4, 1453–1463.

Sambrook, J., Fritsch, E.F., Maniatis, T., 1989. Molecular Cloning, A Laboratory Manual. Cold Spring Harbor Laboratory Press, Cold Spring Harbor.

Schuetz, Y.B., Naik, A., Guy, R.H., Vuaridel, E., Kalia, Y.N., 2005. Transdermal iontophoretic delivery of vapreotide acetate across porcine skin in vitro. Pharm. Res. 22, 1305–1312.

Sugio, S., Kashima, A., Mochizuki, S., Noda, M., Kobayashi, K., 1999. Crystal structure of human serum albumin at 2.5 A resolution. Protein Eng. 12, 439–446.

Worm, A.M., Taaning, E., Rossing, N., Parving, H.H., Clemmensen, O.J., 1981. Distribution and degradation of albumin in extensive skin disease. Br. J. Dermatol. 104, 389–396.

Yu, J., Kalaria, D.R., Kalia, Y.N., 2011. Erbium:YAG fractional laser ablation for the percutaneous delivery of intact functional therapeutic antibodies. J. Control. Release. 156, 53–59.

Yu, J., Dubey, S., Kalia, Y.N., 2018. Needle-free cutaneous delivery of living human cells by Er: YAG fractional laser ablation. Expert Opin. Drug Deliv. 15, 559–566.